Mine Water and the Environment (2019) 38:281–293
https://doi.org/10.1007/s10230-018-00585-y

TECHNICAL ARTICLE

Potential Pollution of Groundwater by Dissolution and Release of Contaminants due to Using Gangue for Backfilling

Wenyue Qi[1,2] · Yanli Huang[1,2] · Hu He[3] · Jixiong Zhang[1,2] · Junmeng Li[1,2] · Ming Qiao[1,2]

Received: 30 July 2017 / Accepted: 26 December 2018 / Published online: 24 January 2019

Abstract

Large quantities of solid wastes, including gangue (waste rock) have been added to the goafs in China's coal mines as backfill. In this study, the mineral and chemical compositions of gangue from the No. 12 coal mine of the Pingdingshan Coal Group were investigated to determine potential pollution concerns, and the behaviour of contaminants in the gangue, such as salts, alkali metals, and alkaline earth metals, was explored using static immersion tests. COMSOL Multiphysics was used to study contaminant migration. The concentration and diffusion distance of metal ions were found to increase over time; this was negatively correlated with gangue particle size. Acidic environments promoted the dissolution of Ca, Fe, Mn, Na, Zn, Pb, and Be, while in alkaline environments, Se dissolution was accelerated.

Keywords Backfill · COMSOL Multiphysics · Metal ions · Migration · X-ray diffraction

Introduction

Gangue, the material mined along with the coal, accounts for about 10–15% of coal production. Gangue is generally considered a solid waste, and is commonly disposed of in piles. By 2014, approximately five billion tons of gangue had accumulated in China. In the large state-owned coal mines, there were around 1500–1700 gangue piles, covering approximately 15,000 ha, occupying more of China's land than any other industrial solid waste. The gangue not only occupies large areas of potentially valuable land, it can damage landforms and vegetation, constrain the harmonious development of the environment and society (Li et al. 2015a, 2017, 2018a), and spread dust and toxic substances, affecting the surface water environment and threatening human health (Bian et al. 2012; Li and Qian 2011; Li et al. 2014a; Zhu 2011). Therefore, this problem is an important environmental concern.

The generalized use of gangue is largely dictated by resource recovery and engineering practice. Using gangue as backfill in goaf accounts for 56% of its total utilisation in China (Liu 2006; Ye et al. 2010). The integrated technology of mechanised solid backfilling of wastes such as gangue (Miao et al. 2010; Miao 2012) effectively controls movement of overlying strata and mitigates coal mining's potential damage to the environment (Huang et al. 2011a, b; Ju et al. 2017; Zha 2011). After being used to fill in the goafs, the gangue can form a compact structure under pressure and compaction imposed by the mining-backfilling support shields (Zhang et al. 2015).

However, gangue backfills are buried in a dark, moist environment protected from the atmosphere for a long time, during which water from overlying aquifers continuously seeps into and through the goafs via water-conducting fractured zones (Li 2013; Qiao et al. 2014, 2016). After the mining and backfilling operations are finished, the gangue will experience a long-term leaching process. Coal gangue may decompose into tiny particles and eventually become suspended solids. Moreover, these particles contain toxic metals and inorganic salts that will dissolve and spread in water (Ilhan et al. 2013; Li et al. 2014b, 2016a, 2018b; Sasaki et al.

Electronic supplementary material The online version of this article (https://doi.org/10.1007/s10230-018-00585-y) contains supplementary material, which is available to authorized users.

✉ Yanli Huang
huangyanli6567@163.com

[1] State Key Laboratory of Coal Resources and Safe Mining, Xuzhou 221116, China

[2] School of Mines, China University of Mining and Technology, Xuzhou 221116, China

[3] School of Resources and Geosciences, China University of Mining and Technology, Xuzhou 221116, China

2002; Xiao et al. 2006; Yang et al. 2014). As these toxic metals and inorganic salts migrate to underlying aquifers, they can pose serious risks of pollution to the down-gradient soils and groundwater environment (Li et al. 2015b, 2016b).

We investigated the potential pollution components of the gangues from the No. 12 coal mine of the Pingdingshan Coal Group. We used X-ray diffraction to qualitatively and quantitatively assess the mineral and chemical compositions of the gangue. Also, static immersion tests were carried out to study the influence of the gangue's particle size and the fluid's pH on the dissolution of contaminants from the gangue. COMSOL Multi-physics was then used to predict the migration of contaminants from the coal gangue backfill.

Material, Methods and Experimental Program

Sample Preparation

Samples were collected from the No. 12 coal mine's gangue piles. Considering the degree of weathering and freshness of the gangues, 24 sampling sites were identified using the serpentine sampling method (Cheng et al. 2013), from the bottom, middle, and top of the gangue piles, which was ≈ 35 m in height and totalled ≈ 200,000 tons. Orthogonal sampling was conducted at each sampling site and then the samples were split using the quartering method. In accordance with the particle sizes used as fill in the goaf area, three representative groups were selected: finer than 15 mm, 15–30 mm, and 30–50 mm (designated A, B, and C, respectively). After that, some large pieces of gangue were crushed into particles less than 50 mm in size to mimic actual applications. Then, the gangues were separated into five groups using several sizing screens: 40–50 mm, 30–40 mm, 20–30 mm, 15–20 mm, and finer than 15 mm. Finally, the grouped samples were mixed within each group and dried before being put into wide-mouth jars as representative samples for use in the experiments.

Gangue Components

An X-ray diffractometer was used for qualitative and quantitative analysis of the gangue according to the standard method of analysis. Contrast analyses were carried out to determine mineral and chemical compositions by matching the diffractograms with various powder diffraction files.

Immersion Tests

Gangues with different particle sizes soaked in water with varying pH values will contribute different contaminant concentrations (Cao et al. 2010; He et al. 2014; Ma et al. 2015). So, experiments were conducted separately in acid, alkaline, and neutral water using three representative samples with the already-specified particle sized groups. According to the standards for identifying the toxicity of wastes by extraction [General Administration of Quality Supervision, Inspection and Quarantine (AQSIQ) 2007], pollution components in suspensions of coal gangues were measured using an inductively coupled plasma-optical emission spectrometer (ICP-AES). According to China's Groundwater Environmental Quality Standards (AQSIQ 2002, 2017), the primary potential components were Fe, Mn, Cu, Zn, Pb, Cd, Hg, alkaline earth metal ions (Be and Ca), an alkali metal ion (Na), a semi-metal (As), and a non-metal (Se).

The test programme outlined in Table 1 was established based on the assumption that particle size and pH were the master driving factors. The gangue samples, 1000 g each, were weighed and then put into large plastic buckets in which distilled water or test solution was then added. The solution was stirred every 6 h, and supernatant liquid was removed every 48 h after the solution had become transparent, until ion precipitation was dynamically balanced. The solution was put into a glass jar, sealed, and labelled.

Results

Mineral and Chemical Compositions

The results of the gangues analysis are shown in Table 2 and Fig. 1. Quartz and kaolinite were the main components, with quartz accounting for 37%. Other components were illite, mixed layers of illite and smectite (I/S mixed-layers), and traces of chlorite, siderite, and pyrite.

The chemical compositions of the gangue are summarised in Table 3. SiO_2 and Al_2O_3 were the main components but the gangues were also rich in alkali metals (Na and K), alkaline earth metals (Be, Mg, and Ca), and sulphides. Additionally, extraction and analysis showed that the gangue

Table 1 Test combinations

Serial number	Test number	Particle size (mm)	pH
1	A-3-5	A (0–15 mm)	5
2	A-3-7		7
3	A-3-9		9
4	B-3-5	B (15–30 mm)	5
5	B-3-7		7
6	B-3-9		9
7	C-3-5	C (30–50 mm)	5
8	C-3-7		7
9	C-3-9		9

Table 2 Material compositions of the gangues in the coal mine (%)

Samples	Quartz	Kaolinite	Illite	Mixed-layer of illite and smectite	Smectite	Chlorite	Feldspar	Calcite	Non-crystal substance	Sum
No.1	37	35	12	6	1	2	1	0.5	4	98.5
No.2	36	35	10	8	0.8	3	0.9	0.4	3	97.1
No.3	38	34	13	5	1.2	1	0.9	0.6	5	98.7
Average	37	34.7	10.7	7.3	1.0	2	0.9	0.5	4	98.1

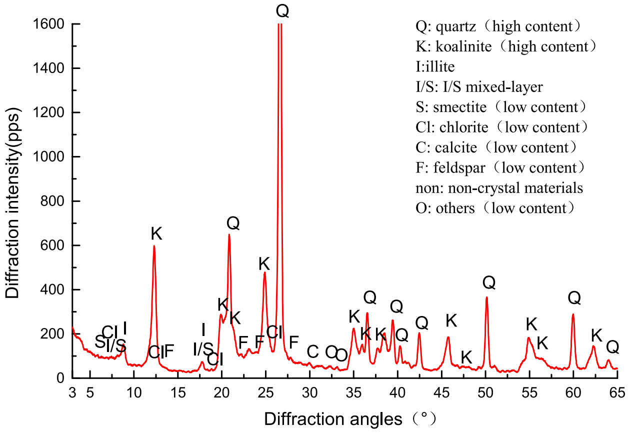

Fig. 1 X-ray diffraction patterns of the gangue samples

contained Fe, Ba, Mn, Cu, Zn, Ti, Pb, Hg, Be, and other elements.

Influence of Particle Size (pH 7)

Particle size affected the concentrations of various ions after neutral solution immersion (Fig. 2). The concentrations of some ions were below their detection limit (as shown in the online resource Table S2). It can be seen that the concentrations of Ca, Na, Fe, Mn, Zn, and Se ions that dissolved changed with time in a similar manner for the differently sized groups. The concentration of released ions increased with immersion time, while the release rate decreased. The concentrations of ions increased rapidly in the initial- (0–4 days) and medium-term (4–10 days), while they gradually steadied in the later stages of immersion.

The ions in the immersion solution were mainly dissolved and oxidised from the minerals in the gangue (Alhaji and Jeng 1992; Dang et al. 1996). The K_{sp} expressing the solubility of the minerals in water are shown in Table 4, from which it is inferred that the low K_{sp} of those minerals caused low concentrations of metal ions (Dang et al. 2001). In comparison, mineral oxidation was the primary factor determining the metal ion concentrations. In addition, some of the dissolved metal ions originated from non-crystalline substances. Per Eqs. 1–6, dissolved oxygen is consumed while ion concentrations stabilize and the rate of dissolution of these minerals gradually decreased (Perry 1995; Xiao 2007).

$$CuFeS_2+\frac{17}{4}O_2(aq)+\frac{5}{2}H_2O \rightarrow 2H^{+}+2SO_4^{\ 2-}+Cu^{2+}+Fe(OH)_3 \quad (1)$$

$$ZnS(s)+2O_2(aq) \rightarrow Zn^{2+}+SO_4^{\ 2-} \quad (2)$$

$$FeS_2+\frac{15}{4}O_2(aq)+\frac{7}{2}H_2O \rightarrow 4H^{+}+2SO_4^{\ 2-}+Fe(OH)_3 \quad (3)$$

$$2FeS_2+7O_2(aq)+2H_2O \rightarrow 2Fe^{2+}+4H^{+}+4SO_4^{\ 2-} \quad (4)$$

$$CaCO_3+H_2CO_3 \rightarrow Ca^{2+}+2HCO_3^{\ -} \quad (5)$$

$$\begin{aligned} &Me-Al-silicate+H_2CO_3+H_2O \\ &\rightarrow nHCO_3^{\ -}+Me^{n+}+Al-silicate \end{aligned} \quad (6)$$

The curves representing the concentrations of released ions were approximately logarithmic. This was a result of various processes: (a) reactive contact is limited by the permeation of water into the gangue; (b) dissolved oxygen gradually reacts with the minerals on the surface, leading to the metal ions diffusing into solution; (c) some metal ions are adsorbed on the gangue surfaces because the gangue contains a certain amount of carbonic matter, which has honeycomb-like micro-pores on its surface and

Table 3 Chemical compositions of the gangue samples (%)

Samples	Na_2O	MgO	Al_2O_3	SiO_2	K_2O	CaO	Fe_2O_3	S	P	Ti	Ba	Mn	Cu	Pb	Zn	Sum
No.1	1.2	1.2	24.3	53.1	1.3	5.4	1.9	0.8	0.03	0.48	0.11	0.09	0.001	0.002	0.007	89.92
No.2	1.4	1.5	26.4	56.2	1.5	5.8	2.4	0.9	0.04	0.43	0.14	0.12	0.001	0.002	0.007	96.84
No.3	1.3	1.1	25.2	53.8	1.7	5.1	2.1	1.1	0.02	0.52	0.12	0.12	0.002	0.004	0.008	92.19
Average	1.3	1.3	25.3	54.4	1.5	5.4	2.1	0.9	0.03	0.47	0.12	0.11	0.001	0.003	0.007	92.94

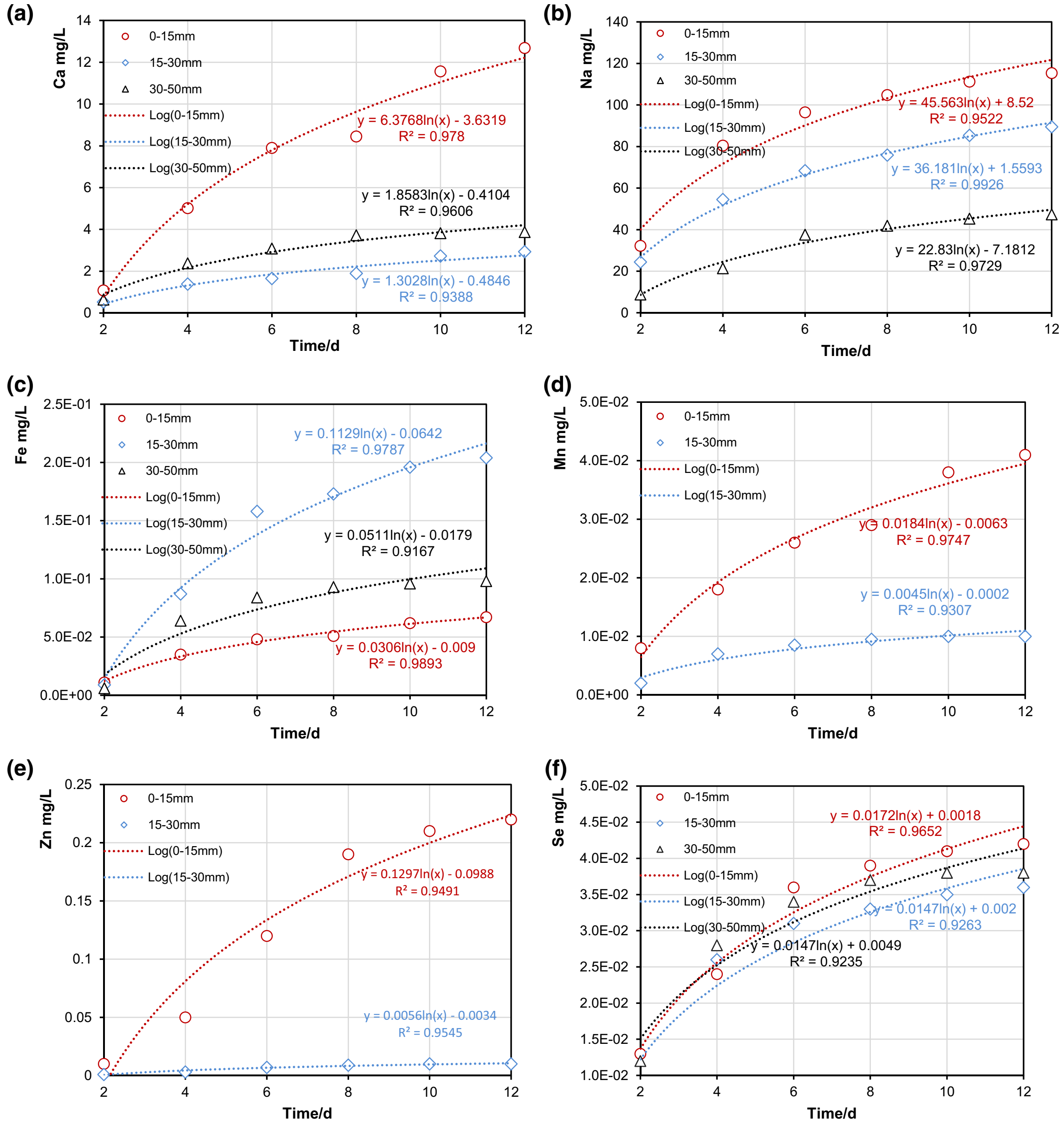

Fig. 2 Concentration of ions released from gangues with different particle sizes during immersion (pH 7): **a** Ca, **b** Na, **c** Fe, **d** Mn, **e** Zn, **f** Se

Table 4 Solubility product constants (K_{sp}) and solubilities of low, and quasi-insoluble minerals (Dang et al. 2001)

Minerals	Siderite	Calcite	Greenockite	Galena	Spalerite	Pyrite
K_{sp}	3.2×10^{-11}	3.8×10^{-9}	1.6×10^{-28}	2.5×10^{-27}	1.6×10^{-24}	6.3×10^{-31}
Solubility (mol/L)	6.554×10^{-5}	6.2×10^{-5}	1.3×10^{-14}	5.0×10^{-14}	1.3×10^{-12}	7.9×10^{-16}

within its lattice structure (Li and Chen 2012; Wang and Li 2014). In addition, hydrate silica gels, aluminium salts, molysites, and aluminium silicate gels with flocculation-adsorption capacity are also formed, which can adsorb small amounts of metal ions (Guo 2010; Hu et al. 2013); and (d) some of the dissolved metals ions undergo reactions to form secondary minerals precipitates, such as $Fe(OH)_3$, $Fe(OH)_2$, $Zn(OH)_2$, and $Cu(OH)_2$ (Zhang 2011). Redox reactions and diffusion are the primary processes during the medium-term, during which adsorption and secondary precipitation reactions were less important. Adsorption and secondary precipitation reactions are the primary reaction processes over a longer time scale, as was observed after 8 days in our experimental systems (Yang and Ji 2016). These processes were obvious from the concentration curves for the Cu ions, which slowly decreased during the later reaction period with adsorption and precipitation.

The concentrations of Ca, Na, Mn, Zn, and Se ions were negatively correlated with particle size. In particular, at pH 7, the concentrations of Ca ions were 12.7, 2.9, and 3.9 mg/L when the particle size of the gangues were 0–15, 15–30, and 30–50 mm, respectively. This shows that increasing the solid–liquid interface area increased the dissolution of the contaminants. It is worth noting that the concentrations of Na, Mn, Ca, and Zn ions in the initial-term and medium-term were significantly influenced by the particle size, while the concentrations of Se ions were only slightly influenced by particle size. In addition, the concentration of Fe ions was greatest when the particle size was between 15 and 30 mm. The release rate data (Table 5) reflect the extent of migration of the ions because acid-soluble and oxidizable metal ions are easily precipitated.

At pH 7, the gradual diffusion of Fe, Mn, Zn, and Se (especially the three metal ions) into the underground aquifer would have a detrimental influence on the groundwater. The concentrations of other metal and metalloid ions (Cu, Pb, Cd, As, and Hg) were generally less than the analytical instrument's detection limits. Therefore, these are unlikely to be of concern.

Influence of Particle Size (pH 5)

The changing concentrations of Ca, Na, Mn, Zn, Cu, Be, and Pb ions are shown in Fig. 3. At pH 5, the concentrations of metal ions increase in different ways. While the concentrations of Fe, Na, and Mn ions increased strongly, those of Ca and Zn increased slightly. In contrast to pH 7, where Cu, Be, and Pb ions had not been released, obvious concentrations were detected at pH 5.

At pH 5, the concentrations of Ca, Na, Mn, Zn, and Cu ions were negatively correlated with the gangue's particle size, whereas the Fe ions were positively correlated with the particle size. However, the Pb and Be ion concentrations were greatest when the particles were between 15 and 30 mm. The concentrations of Na, Mn, Zn, Fe, Pb, and Be ions were significantly affected by particle size, while those of Ca and Cu ions were only slightly affected.

Some metal ions, namely Cu and Pb, precipitated in the acidic environment. The concentrations of other metal ions (Fe, Mn, and Zn) increased, and would probably deteriorate groundwater quality. Other metal and metalloid ions (Cd, As and Hg) were still less than the detection limit.

Influence of Particle Size (pH 9)

The changing concentrations of Ca, Fe, Na, and Se ions are shown in Fig. 4. At pH 9, the concentrations of Ca and Fe ions were less than at pH 7 or pH 5, while the concentrations of Se and Na ions were slightly higher. The alkalinity of the reaction liquid restrained the dissolution or enhanced the precipitation of Ca, Fe, Mn, Zn, Pb, and Be ions, but promoted the release of Se ions, while Na ions were less affected. The Na and Fe concentrations were negatively correlated with the gangue's particle size, while the Ca and Se concentrations were greatest when the particle size was 15–30 mm.

The higher OH^- restrained the concentrations of Fe, Mn, Zn, Pb, Be, and Ca ions and promoted Se dissolution, while Na ions were less affected. The secondary precipitation of hydroxide minerals was facilitated by the higher OH^- concentration. In addition, the higher pH restrained dissolution of carbonate, aluminosilicate, and sulphide minerals. Also, in the alkaline environment, the adsorptive capacity of the gangue mineral surfaces for metal ions was slightly reduced.

At pH 9, it appears that Fe and Se ions would gradually diffuse into the underground aquifer, possibly at concentrations high enough to deteriorate the groundwater quality. The concentrations of Mn, Zn, Cu, Pb, Be, Cd, As, and Hg, were nearly zero, and should not affect groundwater quality.

Mathematical Modelling of the Ion Dissolution

The ion concentrations acquired in the immersion tests were fitted using the least squares method. Linear regression of the measured ion concentrations was performed, with the concentration of each substance as the y-axis, and time as the x-axis. The slope of the fitting line is the average release rate for each ion. The results suggested that the concentrations of ions in the immersion showed a logarithmic relationship with time (Table 6), with: $y_i = a + b\ln(x)$.

Table 5 The average release rate of metal ions(mg/L·h)

Particle size (mm)	Ca	Na	Mn	Zn	Se	Fe
0–15	1.1168	4.5307	0.0033	0.0229	0.0028	0.0052
15–30	0.3023	3.9023	0.0007	0.001	0.0023	0.0188
30–50	0.2334	3.2081	/	/	0.0023	0.0081

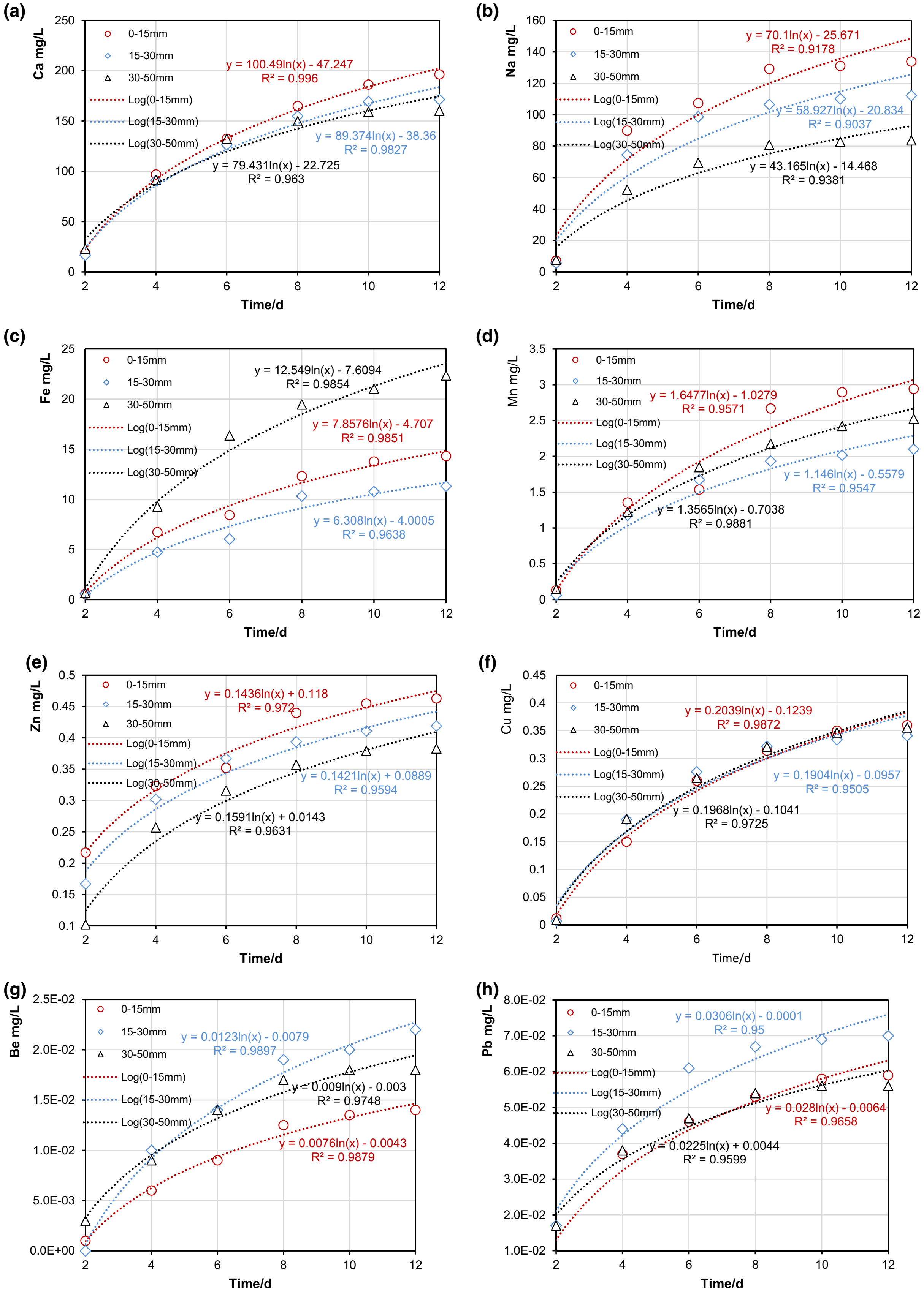

Fig. 3 Concentration of ions released from gangues with different particle sizes during immersion (pH 5): **a** Ca, **b** Na, **c** Fe, **d** Mn, **e** Zn, **f** Cu, **g** Be, **h** Pb

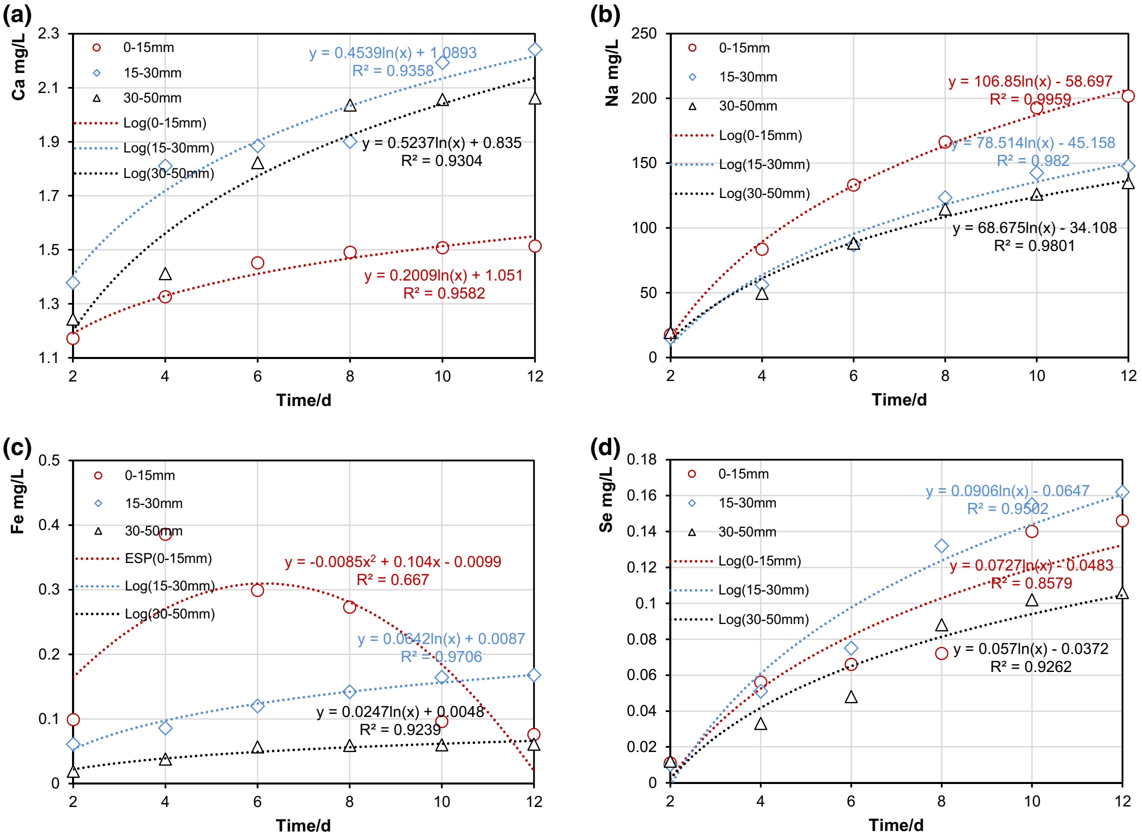

Fig. 4 Concentration of ions released from gangues with different particle sizes during immersion (pH 9) (ESP means polynomial): **a** Ca, **b** Na, **c** Fe, **d** Se

Table 6 Logarithmic relationship of the concentrations at pH 7 with immersion time (day)

ions	Particle size (mm)	Fitted logarithmic curve equation	Goodness of fit
Fe	0–15	$y = 0.0306\ln(x) - 0.0090$	$R^2 = 0.9893$
	15–30	$y = 0.1129\ln(x) - 0.0642$	$R^2 = 0.9787$
	30–50	$y = 0.0511\ln(x) - 0.0179$	$R^2 = 0.9167$
Mn	0–15	$y = 0.0184\ln(x) - 0.0063$	$R^2 = 0.9747$
	15–30	$y = 0.0045\ln(x) - 0.0002$	$R^2 = 0.9307$
Zn	0–15	$y = 0.1297\ln(x) - 0.0988$	$R^2 = 0.9491$
	15–30	$y = 0.0056\ln(x) - 0.0034$	$R^2 = 0.9545$
Se	0–15	$y = 0.0172\ln(x) + 0.0018$	$R^2 = 0.9652$
	15–30	$y = 0.0074\ \ln(x) - 0.0042$	$R^2 = 0.9987$

Numerical Simulation of Ion Migration

Basic Assumptions

Figure 5 shows the mechanisms of groundwater pollution by backfill and gangue piles. The assumptions for describing the migration of metal and metalloid ions in coupled seepage and concentration fields from the gangue backfill are as follows:

1. The gangue fill is regarded as a porous medium with variable saturation;
2. The permeability of the gangue itself is ignored;
3. Continuously seeping gas bubbles and droplets in the pores are ignored; and.
4. The flow of groundwater in the solid stope and floor strata complies with Darcy's linear percolation law.

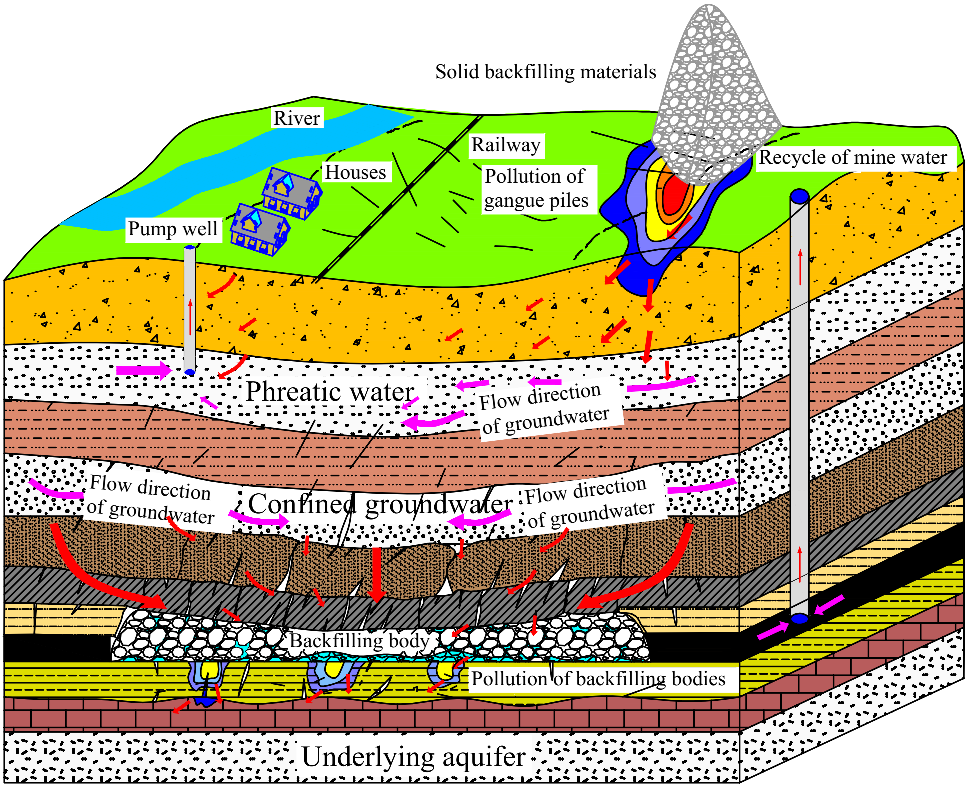

Fig. 5 Interaction between gangue backfilling bodies and mine water

Governing Equations

According to the law of conservation of mass and the above assumptions, the continuity equation of the liquid phase was derived after the representative elementary volume was defined as:

$$\nabla \cdot \left(\rho_w \bar{V}_w\right) = \frac{\partial}{\partial t}\left(S_w \phi \rho_w\right) \tag{7}$$

where ρ_w is the fluid density; $\bar{V}_w$ is the velocity vector, t is the time, S_w is the liquid saturation of the pore space, and ϕ is the porosity.

Substituting the equation of motion $\bar{V}_w = -\frac{\kappa_w}{\eta_w}\nabla \rho_w + \rho_w g z$ into the continuity equation, the basic control equation of seepage through unsaturated media was obtained.

$$-\nabla \cdot \left(\rho_w \kappa \frac{\left(\kappa_r\right)_w}{\eta_w} \nabla\left(\rho_w + \rho_w g z\right)\right) = S_w\left(\rho_w \frac{\partial \phi}{\partial t} + \phi \frac{\partial \rho_w}{\partial t}\right) + \rho_w C_w \frac{\partial \rho_w}{\partial t} \tag{8}$$

where κ_w is the liquid effective permeability, p_w is the liquid pressure, g is the acceleration of gravity, z is the difference in height, $\left(\kappa_r\right)_w$ is the relative permeability, C_w is the moisture capacity, η_w is the dynamic viscosity, and κ is the intrinsic conductivity. The van Genuchten model is adopted in the functions.

The basic equations of multi-component solute transport in saturated medium was derived based on the principle of mass conservation, Fick's law of diffusion, and the theory of fluid dynamic dispersion.

$$\frac{\partial \theta C_i}{\partial t} + \nabla \cdot \left(\theta C_i \bar{V}_i\right) - \nabla \cdot \left(\theta D C_i\right) = \left(Q_S\right)_i \tag{9}$$

where C_i is the component concentration, θ is the rate of water content, $\bar{V}_i$ is the actual velocity of solute components, D is the fluid dynamic dispersion coefficient tensor, and $\left(Q_S\right)_i$ is the source or sink term.

Numerical Model

COMSOL Multiphysics (Faisal and Ali 2016; Nardi et al. 2014; Yeboah et al. 2014) was used to predict ion migration from the coal gangue backfill. We used the 13,080 working face of the Pingdingshan mine as the research site, where the length of the working face is 150 m, the width of the section coal pillar is 25 m, the seam thickness is 5 m, and the thickness of the floor strata is 20 m. The geometric model was divided into free triangulation with Lagrangian secondary units, and the filling body was localized. The model consisted of a complete grid of 4785

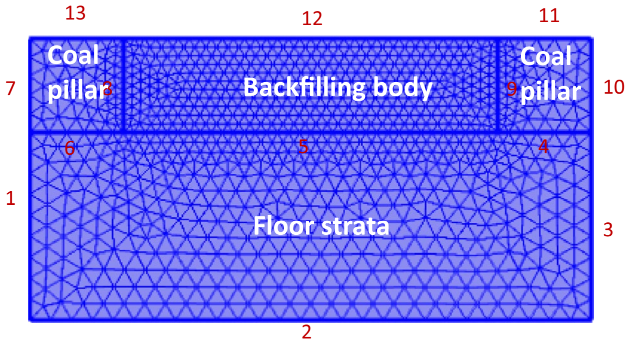

Fig. 6 Finite element model of backfill mining stope

domain units and 469 boundary elements (Fig. 6), illustrating a unit cell sketch with 13 boundaries. The particle size of the gangue material was set to 5 mm < d < 50 mm. The calculated parameters of the seepage field model in the simulation are summarised in Table 7 and Online Resource Table S1. Referring to Fig. 6, the boundary conditions were:

1. For the seepage field, boundary 12 was selected as the mass flow condition, while boundary 8 and 9 were selected as permeable stratum conditions.
2. For transport of diluted components in porous media, boundary 12 was selected as the mass flow condition, while boundary 2 was selected as the outflow condition.

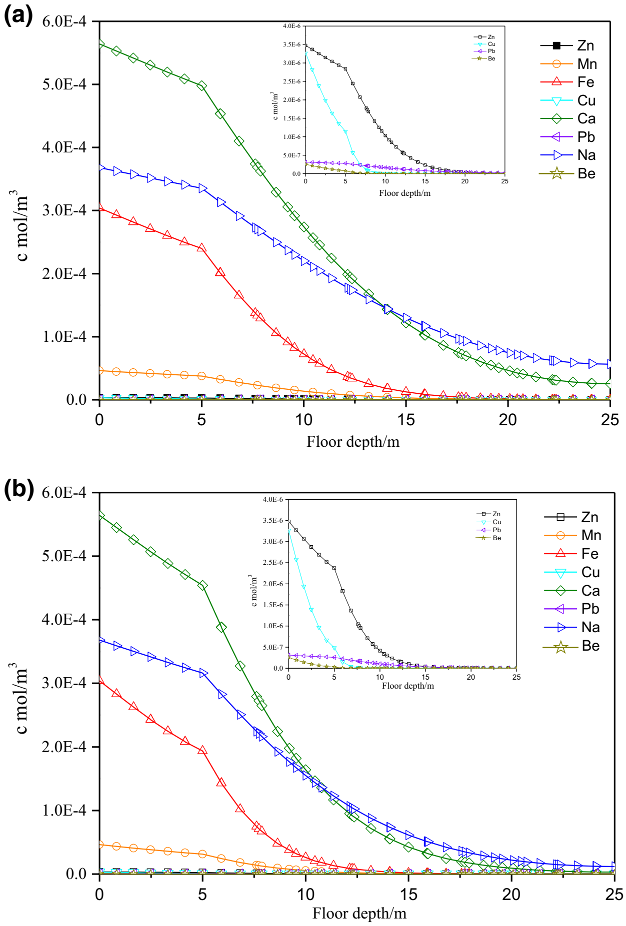

Fig. 7 Distribution of ion diffusion: **a** 10 years, **b** 20 years

Results and Discussion

Selecting the A-3-5 sample test (pH 5, 0–15 mm; see Table 3) and fitting the results for the concentration boundary, the migration (ion concentration distribution) of the eight metal components (Fe, Mn, Cu, Zn, Pb, Ca, Na, Be) was simulated for 20 years.

The concentration distributions of the different ions after 10 and 20 years are shown in Fig. 7 and Online Resources Figs. S1, S2. The ion concentrations decreases along with the increase in the floor depth, indicating that diffusivity decreases with the increasing depth, because the ions are continuously adsorbed by the floor material. In addition, the pressure gradient continues to decrease, inhibiting the downward diffusion of ions. The diffusion capacity of ions is in accordance with the release rate of the experimental ions: Ca > Na > Fe > Zn > Mn > Cu > Pb > Be. The concentration of ions at a constant depth continuously increases over time, forming higher concentration gradients. This promotes further downward diffusion of ions into the floor.

The migration and diffusion distance of ions in the floor change over time (Fig. 8). The ion diffusion distance increases with time, growing rapidly from 2 to 10 years, after which it steadies. The relationship between the ion diffusion distance and time can be described by an exponential function, $y = a \times \exp(-x/b) + c$

Table 7 Calculation parameters of seepage field model in simulation area

Parameters	θ_s	θ_r	K_s	ρ_w	V-G (α)	V-G (n)
Units	1	1	m (day)	kg/m^3	1/m	1
d < 15	0.3201	0.0389	0.5922	1000	2.94	1.8089
15 < d < 30	0.3132	0.0400	0.6977	1000	3.02	1.9139
30 < d < 50	0.3024	0.0411	0.7965	1000	3.21	2.0066

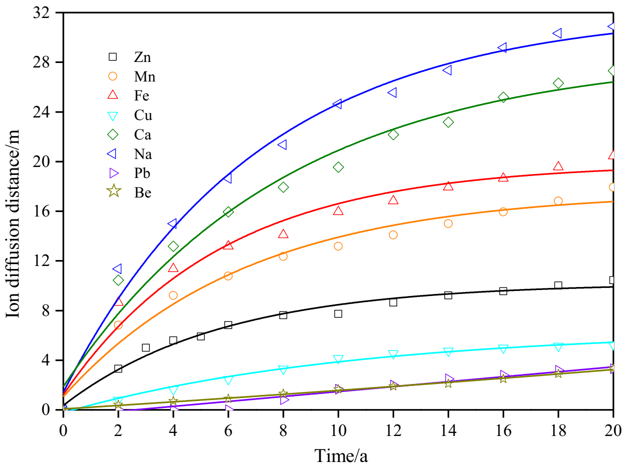

Fig. 8 Ion diffusion distance as a function of time

Samples A-3-5, B-3-5, and C-3-5 were chosen to illustrate the migration and diffusion of Cu and Ca ions for different particle sizes at pH 5 (Fig. 9). With increasing time, the ion concentrations at a single depth continuously increases. The ion concentrations and diffusion distance were negatively correlated with the particle size. The smaller the particles, the higher the concentrations of ions, and the further the diffusion distance. The dissolution rate was consistent with the initial and final dissolution concentration of the ions from the immersion test.

Samples B-3-5, B-3-7, and B-3-9 (15–30 mm particle size fraction) were chosen to illustrate the effect of pH on the migration and diffusion of Fe and Ca ions (Fig. 10). The effect of pH on the ion diffusion concentration is remarkable. Although the initial concentration varies greatly, the ion diffusion distance is roughly negatively correlated with pH. The lower the pH, the higher the initial release concentration, the faster the ions diffuse, and the larger the concentration gradient.

Conclusions

1. The concentrations of metal ions released were negatively correlated with the gangue particle size. Smaller particles exposed more specific surface area of the

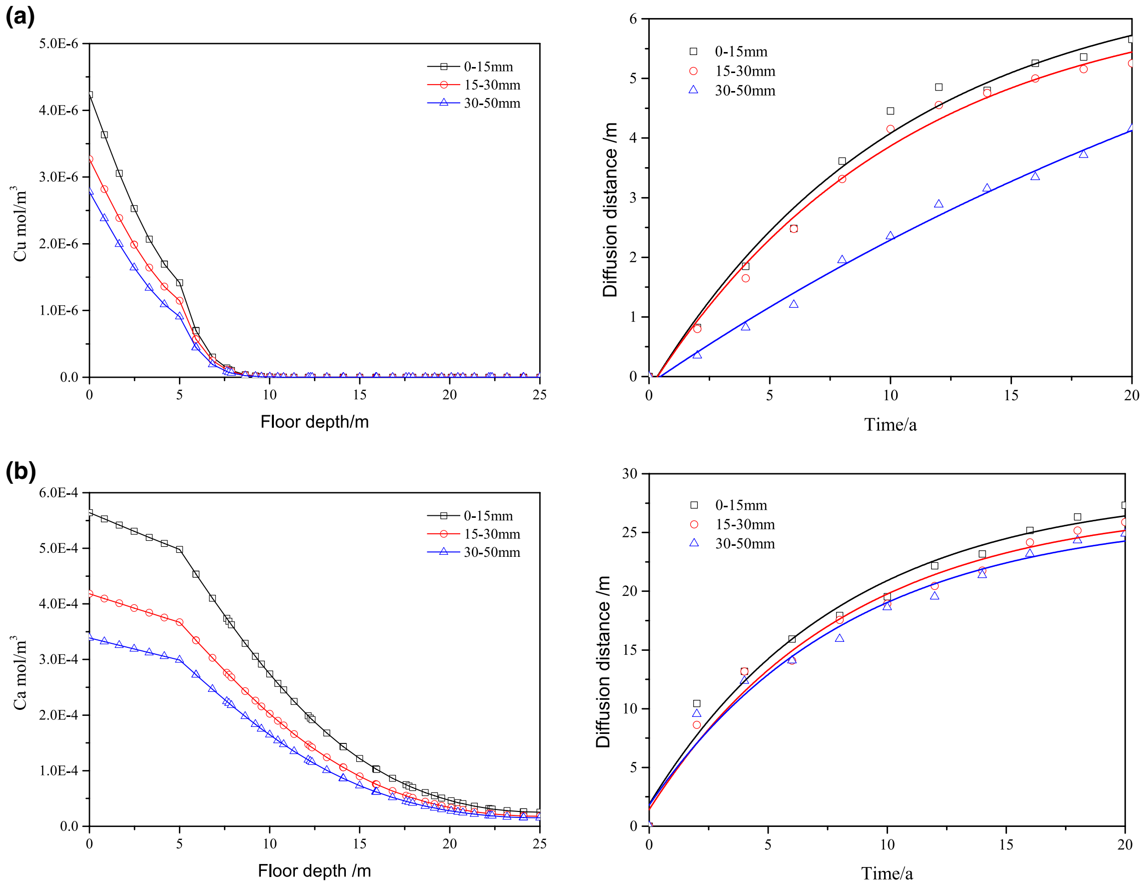

Fig. 9 Migration and diffusion from differently sized particles at pH 5: **a** Cu, **b** Ca

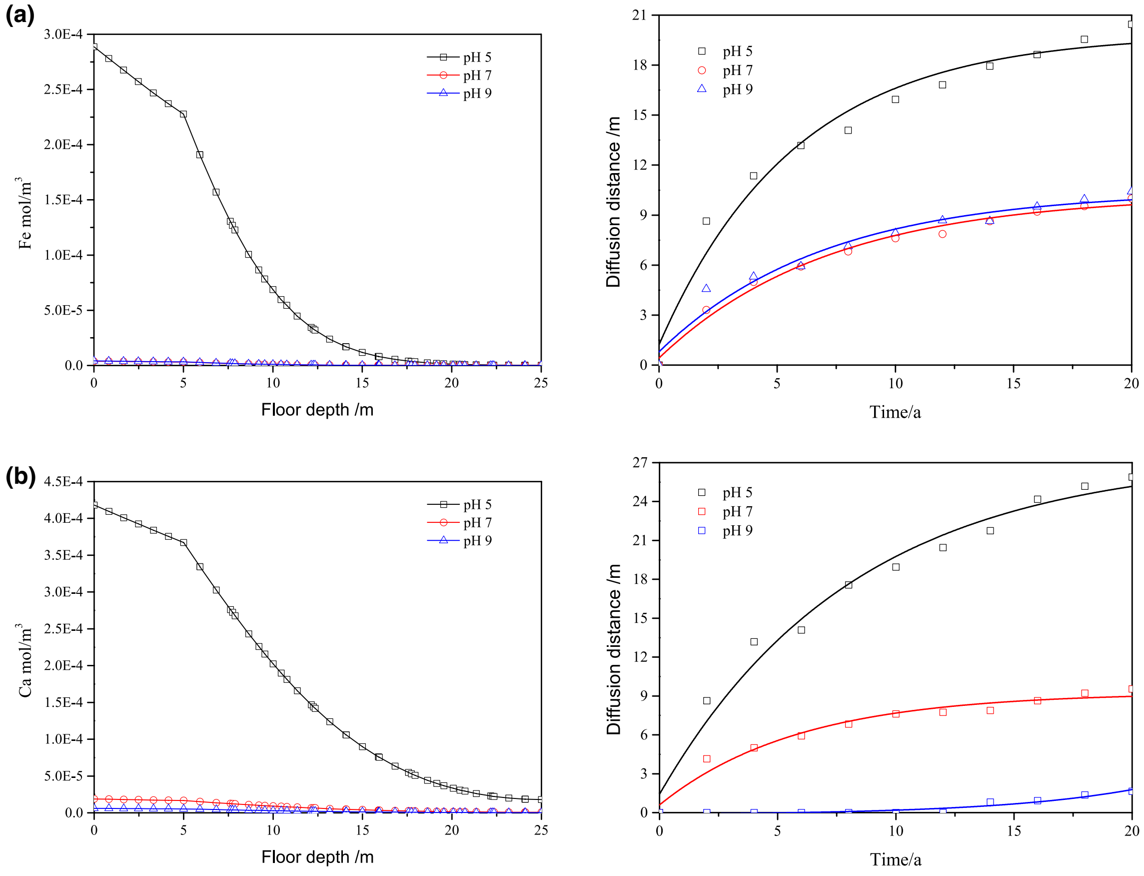

Fig. 10 Migration and diffusion at varied pH for 15–30 mm particle size fraction: **a** Fe, **b** Ca

gangue to water, and generated higher concentrations of metal ions. The total dissolution release rate was negatively correlated with particle size. The smaller the particle size, the quicker the dissolution release rate of the metal ions. However, we have no sound explanation why Fe dissolution increased with increasing particle size. We will be conducting more research to find out why.

2. Mine operators can influence the goaf water at its source, its pH, and the gangue particle size. Constructing a barrier layer (aquifuge) at the ground level of the goaf will reduce direct contact with the groundwater. An effective method to improve the filling rate is to restrain the water source by controlling the height of the water-conducting fractured zones. Also, suitable materials should be selected to neutralize the mine water without generating new contaminants. In addition, it would be beneficial to avoid crushing the gangue too fine, which will also improve the bearing capacity of the backfill. A slurry that can adsorb metal ions should be injected into the floor strata (see Fig. 6) to form an artificial aquifuge and protect the groundwater.

Acknowledgements Financial support for this work was provided by the Fundamental Research Funds for the Central Universities (2017XKZD13).

References

Bian Z, Miao X, Lei S, Chen SE, Wang W, Struthers S (2012) The challenges of reusing mining and mineral-processing wastes. Science 337(6095):702–703. https://doi.org/10.1126/science.1224757

Cao YQ, Zhang SS, Liu HH, Wei L (2010) Leaching characteristics of heavy metals in coal gangue in both dynamic leaching and static immersion. J Hebei Univ Eng 27(1):76–80 **(in Chinese)**

Cheng F, Cheng JP, Sang HC, Yu JL, Xi L, Pi SS (2013) Assessment and correlation analysis of heavy metals pollution in soil of Dajinshan Island. Environ Sci 34(3):1062. https://doi.org/10.13227/j.hjkx.2013.03.033

Dang Z, Wan GJ, LI DR, Watts SF, Haigh M (1996) Kinetics of coal mine spoil—water interaction—II. Mineralogical study on trace metal elements in coal gangue. Sci Chin D 26(1):16–20 **(in Chinese)**

Dang Z, Liu CQ, Li Z (2001) Experimental simulation of chemical activity of heavy metals in coal gangue. J S Chin Univ Tech Nat Sci 29(12):1–5 **(in Chinese)**

Faisal AAH, Ali ZTA (2016) Groundwater protection from lead contamination using granular dead anaerobic sludge biosorbent as permeable reactive barrier. Desalin Water Treat 57(9):3891–3903. https://doi.org/10.1080/19443994.2014.990928

General Administration of Quality Supervision, Inspection and Quarantine (2002) Environmental quality standards for surface water. GB 3838-2002. Standards Press of China, Beijing

General Administration of Quality Supervision, Inspection and Quarantine (2007) Identification standards for hazardous wastes—identification for extraction toxicity. In: GB5085.3-2007. Standards Press of China, Beijing

General Administration of Quality Supervision, Inspection and Quarantine (2017) Standard for groundwater quality. GB/T 14848-2017. Standards Press of China, Beijing

Guo C (2010) Research progress of coal gangue adsorbent. China Sci Technol Expo (34): 378–379 **(in Chinese)**

He B, Zhang Y, Li XD (2014) Research on experimental dissolution of coal gangue main pollution components. Bull Chin Ceram Soc 33(9):2217–2222 **(in Chinese)**

Hu J, Hu ND, Lian ML, Miao YJ (2013) Progress of application of coal gangue in the wastewater treatment. Yunnan Chem Technol 40(02):22–25 **(in Chinese)**

Huang Y, Zhang J, Zhang Q, Nie S (2011a) Backfilling technology of substituting waste and fly ash for coal underground in china coal mining area. Environ Eng Manag J 10(6):769–775

Huang Y, Zhang J, An B, Zhang Q (2011b) Overlying strata movement law in fully mechanized coal mining and backfilling longwall face by similar physical simulation. J Min Sci 47(5):618–627

Ilhan S, Kalpakli AO, Kahruman C, Yusufoglu I (2013) The investigation of dissolution behavior of gangue materials during the dissolution of scheelite concentrate in oxalic acid solution. Hydrometallurgy 136(4):15–26. https://doi.org/10.1016/j.hydromet.2013.02.013

Jeng A (1992) Weathering of some Norwegian alum shales II. Laboratory simulations to study the influence of aging, acidification and liming on heavy metal release. Acta Agr Scand B 42(2):76–87. https://doi.org/10.1080/09064719209410203

Ju F, Huang P, Guo S, Xiao M, Lan L (2017) A roof model and its application in solid backfilling mining. Int J Min Sci Technol 27 (1):139-143

Li J (2013) Evolution mechanism and control of water-flowing fracture with gangue backfill under aquifer in coal mine. China University of Mining and Technology, Xuzhou **(in Chinese)**

Li D, Chen HJ (2012) Study development of wastewater adsorbent prepared by coal gangue. J Luoyang Inst Sci Tech 22(03):6–9, 15 **(in Chinese)**

Li P, Qian H (2011) Human health risk assessment for chemical pollutants in drinking water source in Shizuishan city, northwest China. Iran J Env Hlth Sci Eng I 8(1):41–48

Li H, Sun H, Tie X, Xiao X (2006) Dissolution properties of calcined gangue. J Univ Sci Tech Beijing Min Metal Mater 13(6):570–576 **(in Chinese)**

Li P, Wu J, Qian H, Lyu X, Liu H (2014a) Origin and assessment of groundwater pollution and associated health risk: a case study in an industrial park, northwest China. Environ Geochem Health 36(4):693–712. https://doi.org/10.1007/s10653-013-9590-3

Li P, Qian H, Howard KWF, Wu J, Lyu X (2014b) Anthropogenic pollution and variability of manganese in alluvial sediments of the yellow river, Ningxia, northwest China. Environ Monit Assess 186(3):1385–1398. https://doi.org/10.1007/s10661-013-3461-3

Li P, Qian H, Howard KWF, Wu J (2015a) Building a new and sustainable "Silk Road economic belt". Environ Earth Sci 74(10):7267–7270. https://doi.org/10.1007/s12665-015-4739-2

Li P, Qian H, Howard KWF, Wu J (2015b) Heavy metal contamination of yellow river alluvial sediments, northwest China. Environ Earth Sci 73(7):3403–3415. https://doi.org/10.1007/s12665-014-3628-4

Li P, Wu J, Qian H, Zhang Y, Yang N, Jing L, Yu P (2016a) Hydrogeochemical characterization of groundwater in and around a wastewater irrigated forest in the southeastern edge of the Tengger Desert, northwest China. Expos Health 8(3):331–348. https://doi.org/10.1007/s12403-016-0193-y

Li P, Wu J, Qian H, Zhou W (2016b) Distribution, enrichment and sources of trace metals in the topsoil in the vicinity of a steel wire plant along the Silk Road economic belt, northwest China. Environ Earth Sci 75(10):1–16. https://doi.org/10.1007/s12665-016-5719-x

Li P, Qian H, Zhou W (2017) Finding harmony between the environment and humanity: an introduction to the thematic issue of the Silk Road. Environ Earth Sci 76(3):105. https://doi.org/10.1007/s12665-017-6428-9

Li P, Tian R, Liu R (2018a) Solute geochemistry and multivariate analysis of water quality in the Guohua phosphorite mine, Guizhou province, China. Expos Health. https://doi.org/10.1007/s12403-018-0277-y

Li P, Wu J, Tian R, He S, He X, Xue C (2018b) Geochemistry, hydraulic connectivity and quality appraisal of multilayered groundwater in the Hongdunzi coal mine, northwest China. Mine Water Environ 37(2):222–237. https://doi.org/10.1007/s10230-017-0507-8

Liu D (2006) Research on environmental effect and comprehensive utilization of coal-waste rocks. J Meteorol Environ 3:60–62 **(in Chinese)**

Ma D, Bai H, Chen Z, Pu H (2015) Effect of particle mixture on seepage properties of crushed mudstones. Transp Porous Med 108(2):257–277. https://doi.org/10.1007/s11242-015-0473-1

Miao XX (2012) Progress of fully mechanized mining with solid backfilling technology. J Chin Coal Soc 37(8):1247–1255 **(in Chinese)**

Miao X, Zhang J, Guo G (2010) Method and technology of fully-mechanized coal mining with solid waste filling. China University of Mining and Technology Press, Xuzhou **(in Chinese)**

Nardi A, Idiart A, Trinchero P, Vries LMD, Molinero J (2014) Interface COMSOL-PHREEQC (ICP), an efficient numerical framework for the solution of coupled multiphysics and geochemistry. Comput Geosci 69(4):10–21

Perry DL (1995) Handbook of inorganic compounds. World Publishing, New York City

Qiao W, Li W, Zhang X (2014) Characteristic of water chemistry and hydrodynamics of deep karst and its influence on deep coal mining. Arab J Geosci 7(4):1261–1275. https://doi.org/10.1007/s12517-013-0899-0

Qiao W, Li W, Li T, Chang J, Wang Q (2016) Effects of coal mining on shallow water resources in semiarid regions: a case study in the Shennan mining area, Shaanxi, China. Mine Water Environ 36(1):1–10. https://doi.org/10.1007/s10230-016-0414-4

Sasaki K, Haga T, Hirajima T, Kurosawa K, Tsunekawa M (2002) Distribution and transition of heavy metals in mine tailing dumps. Mater Trans 43(11):2778–2783

Wang D, Li Q (2014) Research progress in coal gangue modification. Mod Chem Ind 34(8):50–52 **(in Chinese)**

Xiao LP (2007) Study on pollution laws of coal gangue leaching solution to groundwater system. Liaoning Eng Tech C **(in Chinese)**

Xiao LP, Liang B, Lu H, Bi Y, Zhang CC, Di J (2006) Releasement of contaminants within coal gangue based on soaking experiment—a case study of coal gangue in Xinqiu coal mine, Fuxin. Chin J Geol Haz Contr 17(2):151–150 **(in Chinese)**

Yang Y, Ji H (2016) A study on chemical forms and leaching characteristics of trace elements in coal gangue from xinhua coal mine in Guizhou province, China. Earth Environ 44(1):36–46 **(in Chinese)**

Yang J, Tang Y, Yang K, Rouff AA, Elzinga EJ, Huang JH (2014) Leaching characteristics of vanadium in mine tailings and soils near a vanadium titanomagnetite mining site. J Hazard Mater 264(2):498–504. https://doi.org/10.1016/j.jhazmat.2013.09.063

Ye JW, Shen GD, Lu L (2010) Hazards and comprehensive utilization of coal gangue. Chin Resour Comp Utiliz 28(05):32–34 **(in Chinese)**

Yeboah S, Akiti TT, Fletcher JJ (2014) Numerical modeling of radionuclide migration through a borehole disposal site. Springerplus 3(1):155. https://doi.org/10.1186/2193-1801-3-155

Zha J (2011) Theory and application of subsidence control for solid backfilling mining. China University of Mining and Technology Press, Xuzhou **(in Chinese)**

Zhang ML (2011) Utilization of fly ash for remediation of heavy metals from acid coal waste leachate. J Chin Coal Soc 36(4):654–658 **(in Chinese)**

Zhang Q, Zhang J, Tai Y, Fang K, Yin Y (2015) Horizontal roof gap of backfill hydraulic support. J Centr South Univ 22(9):3544–3555. https://doi.org/10.1007/s11771-015-2894-y

Zhu K (2011) Environmental hazards and comprehensive utilization of coal gangue in sustainable development. Arch Mikrobiol 60(2):1–4. https://doi.org/10.1109/icbbe.2011.5781478